University of Wollongong
Research Online

Faculty of Engineering - Papers (Archive)

Faculty of Engineering and Information Sciences

1-1-2012

Magnetic propulsion of a spiral-type endoscopic microrobot in a real small intestine

Hao Zhou
University of Wollongong, hz467@uowmail.edu.au

Gursel Alici
University of Wollongong, gursel@uow.edu.au

Trung Duc Than
University of Wollongong, dtt581@uowmail.edu.au

Weihua Li
University of Wollongong, weihuali@uow.edu.au

Sylvain Martel
Ecole Polytechnique de Montreal, sylvain.martel@polymtl.ca

Follow this and additional works at: https://ro.uow.edu.au/engpapers

 Part of the Engineering Commons

https://ro.uow.edu.au/engpapers/5275

Recommended Citation

Zhou, Hao; Alici, Gursel; Than, Trung Duc; Li, Weihua; and Martel, Sylvain: Magnetic propulsion of a spiral-type endoscopic microrobot in a real small intestine 2012, 63-68.
https://ro.uow.edu.au/engpapers/5275

Research Online is the open access institutional repository for the University of Wollongong. For further information contact the UOW Library: research-pubs@uow.edu.au

The 2012 IEEE/ASME International Conference on
Advanced Intelligent Mechatronics
July 11-14, 2012, Kaohsiung, Taiwan

Magnetic Propulsion of a Spiral-type Endoscopic Microrobot in a Real Small Intestine

Hao Zhou, Gursel Alici, Trung Duc Than, Weihua Li and Sylvain Martel

Abstract— **This paper reports on the magnetic propulsion of a spiral-type endoscopic mircorobot in a real small intestine. Magnetic modeling was carried out to design and commission an external electromagnetic system, which wirelessly provides power to the robotic agent. The capsules with different spiral structures were magnetically propelled inside a segment of porcine small intestine. From the results, it is shown that the propulsive velocities of the tested capsules are in the range of 2.5 ~ 35 mm/s when rotating frequencies varying between 1 ~ 5 Hz are applied. Among all the capsules prepared for this study, the capsule No. 5, with one spiral and a helical angle of 20° and spiral height of 1 mm, shows the best performance. The effects of the spiral parameters, such as helical angle, number of spirals and spiral height, are evaluated by using the propulsion velocity and the slip ratio as the evaluation criteria.**

I. Introduction

Minimally invasive medicine has been a recent trend for providing health care with minimal trauma, lower pain, fewer complications, improved recovery quality and duration, as well as reduced costs [1]. One of the greatest achievements of such is the invention of a wireless capsule endoscope (WCE) [2], the device capable of exploring the entire gastrointestinal (GI) tract including the small intestine where traditional endoscope can hardly access. It is proved that WCE is quite helpful to the diagnosis of many GI diseases such as bleeding and celiac disease, most of which take place in the small bowel [3]. Moreover, it is widely believed that the further development can make WCE a more exciting and powerful medical tool in the near future, carrying out both diagnostic and therapeutic tasks, such as non-invasive GI surgery and targeted drug delivery [4, 5].

Currently, the commercial capsules still rely on the visceral peristalsis and gravity to move inside the GI tract. In order to realize those promising applications, a robotic capsule is required to replace this passive locomotion and acquire the ability of controllable movements. Presently, two major schemes have been adopted to exploit feasible locomotion mechanisms for WCE. The internal approaches [6, 7, 8, 9, 10] place energy source, e.g., micro batteries, and locomotion modules on board, offering relatively precise movement control. The external approaches generally utilize an external magnetic field, to propel a capsule integrated with a magnetic part embedded along the GI tract. Compared to the former, a magnetically propelled capsule appears more advantageous due to saving much in-house space and no issues about the duration of a power supply, which are the primary issues for robots in micro or even smaller size.

In our previous work, magnetic propulsion was conducted by providing the magnetic capsule with a direct pulling force, which was induced by an external magnetic gradient field [11]. Direct pulling is a popular and straight-forward method to obtain magnetic propulsion [12, 13]. Another feasible method is to generate a rotational magnetic field so that a torque can be induced and exerted on the magnetic capsule for actuation. Once a spiral structure is attached to the robot's surface, the rotational motion can be transformed to a linear movement because of the contact between the spiral structure and the inner environment of the GI tract [14, 15]. Compared to the former one, this method appears more promising to offer wireless propulsion since it is relatively easier to generate a magnetic field with high field intensity rather than generate one with high field gradients over long distances [1].

In this study, a magnetic propulsion system is built to provide active locomotion to a spiral-type microrobot based on an endoscopic capsule. Some theories of magnetism were reviewed and magnetic modeling was conducted to predict the magnetic field's distribution for helping the design and construction of the external electromagnetic system. Then, the capsules with different spiral structures were magnetically propelled inside a real intestinal tract. A sample of the small intestine excised from a pig was used for the in-vitro experiments since porcine small intestine is reportedly similar to a human being's with regards to biomechanical and tribological properties [16]. The results are presented to demonstrate that the propulsive velocities are in the range of 2.5 ~ 35 mm/s when a rotating frequency between 1 ~ 5 Hz is applied. Among all the fabricated capsules in this study, the capsule No. 5, with one spiral and helical angle of 20° and spiral height of 1 mm, shows the best performance. The effects of the spiral parameters, e.g., helical angle, number of spirals and spiral height, are studied by analyzing the

This work has been supported by the funds in Intelligent Nano-Tera Systems Research Laboratory of University of Wollongong.

H. Zhou (hz467@uowmail.edu.au), T. D. Than (dtt581@uowmail.edu.au) and W. Li (weihuali@uow.edu.au) are with the School of Mechanical, Materials and Mechatronic Engineering, University of Wollongong, New South Wales, 2522, Australia.

S. Martel is with the Department of Computer and Software Engineering, and the Institute of Biomedical Engineering, Polytechnique de Montréal, University of Montréal, Montréal, Canada.

G. Alici (Corresponding author) is with the School of Mechanical, Materials and Mechatronic Engineering, and ARC Centre of Excellence for Electromaterials Science , University of Wollongong, New South Wales, 2522, Australia (e-mail: gursel@uow.edu.au).

propulsive velocity and the slip ratio, in order to provide much-needed reference data for the optimization of a spiral-type endoscopic capsule propelled with magnetic actuation.

II. MAGNETIC MODELING

A. Modeling for Distribution of a Magnetic Field

Magnetic torque is caused by the misalignment of the internal magnet's magnetization and the external magnetic field's direction, determined by the following equations [17]:

$$\tau = VM \times B, \quad (1)$$

$$B = \mu_0 \mu_R H, \quad (2)$$

where τ is magnetic torque, V and M indicate the volume and magnetization of the internal magnet, respectively, B and H denote magnetic flux density and field intensity of the external magnetic field, respectively, μ_0 is free-space permeability, equal to $4\pi\times10^{-7}$ H m^{-1} and μ_R is the relative permeability of the environment.

Generally, a permanent magnet (PM) is used as the magnetic part integrated into the robotic capsule. The volume and magnitude of magnetization are almost fixed. Both μ_0 and μ_R hardly change, either. Therefore, to find the maximum torque the microrobot can receive, it is vital to find the distribution of the external magnetic field.

Both PMs and electromagnets can act as the power source. The former is able to produce higher magnetic fields in a smaller form whereas the latter performs better in the control of field strength and direction. When dealing with medical applications, accuracy and safety are always at a premium. Therefore, electromagnets appear advantageous in this aspect. The Biot-Savart Law, illustrated as follows, shows the relationship between electric current and magnetic field intensity.

$$\delta H = \frac{1}{4\pi r^2} i\delta l \times u, \quad (3)$$

where i is the electric current, r is the radial distance from the wire element to the position of interest, l is the wire's length, u is a unit vector along the radial direction [17].

To obtain precise and stable control of magnetic actuation, a dominant uniform magnetic field is required, which can be realized by a Helmholtz coil. A basic Helmholtz coil is comprised of two coaxial coils with identical radius and identical current direction, separated with a distance equal to the radius of the coils. For a circular Helmholtz coil, the magnetic field along the axis can be calculated by

$$H = \frac{inr^2}{2}\left(\frac{1}{\left[r^2+\left(\frac{d}{2}-z\right)^2\right]^{\frac{3}{2}}}+\frac{1}{\left[r^2+\left(\frac{d}{2}+z\right)^2\right]^{\frac{3}{2}}}\right), \quad (4)$$

where n is the number of turns of the coils, d is the gap between the pair, and z is the displacement on the axis.

The other approach to get the distribution of the magnetic field is to use the finite element (FE) analysis. With this method, the magnetic field intensity of each point within the computational domain can be numerically calculated and the results can be depicted in a contour plot straightforwardly. In addition to magnetostatic simulations, the FE method can perform transient analysis as well, enabling the illustration of a time-varying (low frequency) electromagnetic field.

In this study, the FE analysis is performed by a commercial program, Maxwell 13. It is a powerful program to numerically predict magnetic fields from both PMs and electromagnets by using Maxwell's equations and the introduction of magnetic scalar potential [18]. A Newton-Raphson iterative algorithm is adopted for the solution process.

B. Validation of the magnetic models

Both theoretical calculations and FE numerical method are presented to predict the distribution of a magnetic field, especially the one induced by Helmholtz coils. To validate the models, the magnetic flux densities along the axis of one Helmholtz coil were measured. The internal and external diameters of each coil are 180 mm and 330 mm, respectively. The coil length is 87 mm and the number of turns is 1000. The same dimensions were used in the theoretical calculations and the FE analysis. The current was set as 1 A, provided by a DC power supply.

For the Helmholtz configuration in the FE simulations, the number of elements for the computational domain was around 260, 000. The comparisons between the modeling results and experimental data are illustrated in Fig. 2. From the graph, it is observed that both the theoretical calculations and simulation results are reasonably consistent with the experimental data, which proves the feasibility of the models as the tools to predict the magnetic field distribution.

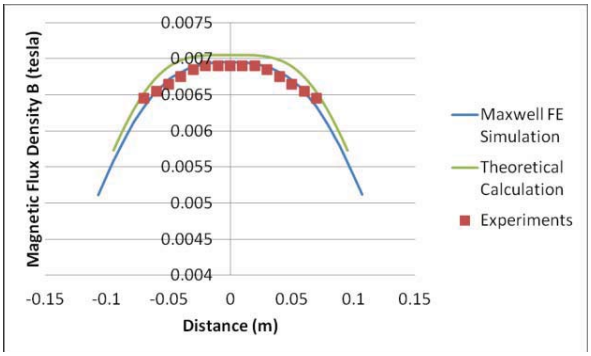

Fig. 2. Validation of magnetic models.

C. Circular vs. Square Helmholtz Coils

Currently, circular and square Helmholtz coils are widely used to generate uniform magnetic fields. The interest in polygonal coil systems of high homogeneity is also rising. Therefore, it is necessary to analyze the performance of a polygonal coil so that we can decide which shape of coil is supposed to be used for the Helmholtz coil system.

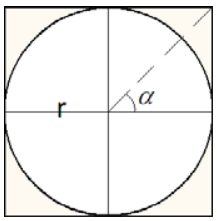

Fig. 3. Diagram of a polygonal coil.

Since the distance between the center and each side is identical, the magnetic field intensity H should be equal to the contribution from one side multiplied by the number of sides. Therefore, the magnetic field intensity at the center of a polygonal coil can be calculated by

$$H = n\int_{-\pi/n}^{\pi/n} \frac{i}{4\pi r}\cos\alpha d\alpha = \frac{ni}{2\pi r}\sin\frac{\pi}{n}, \quad (5)$$

where, n is the number of sides, which is no smaller than 3.

When n trends to infinitely large, the magnetic field H approaches the maximum, identical to the value from a circular coil, shown in both Eq. 6 and Fig. 4.

$$\lim_{n\to+\infty} \frac{ni}{2\pi r}\sin\frac{\pi}{n} = \frac{ni}{2\pi r}\cdot\frac{\pi}{n} = \frac{i}{2r}. \quad (6)$$

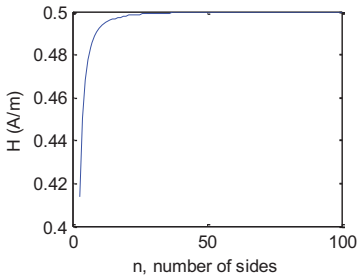

Fig. 4. The relationship between H (at the center) and the number of sides for a polygonal coil, i = 1 and r = 1 assumed.

Three-dimensional FE simulations were also performed to compare the performance of circular and square Helmholtz coils. Fig. 5 shows the magnetic distributions at the middle plane of the two types of Helmholtz coils with the comparable dimensions and identical current input. From the graph, it can be seen that the circular one can generate higher magnetic field intensity.

Based on the outcome of this modeling analysis, it is better to choose circular rather than polygonal coils for the external electromagnetic system due to the desire for higher magnetic field intensity.

D. Rotating Magnetic Field and Multiple-axial Helmholtz Coils

In order to make the magnetic capsule constantly spin, a rotating magnetic field is required. To generate this kind of field, at least two Helmholtz coils are needed. They are placed in an axial orthogonal position and imposed two way of sinusoidal current with the same magnitude and π/2 phase difference. However, this biaxial Helmholtz coil system can only make the spiral-type capsule travel forward or backward and cannot change the moving direction freely due to the lack of the ability to change the rotational plane. A triaxial

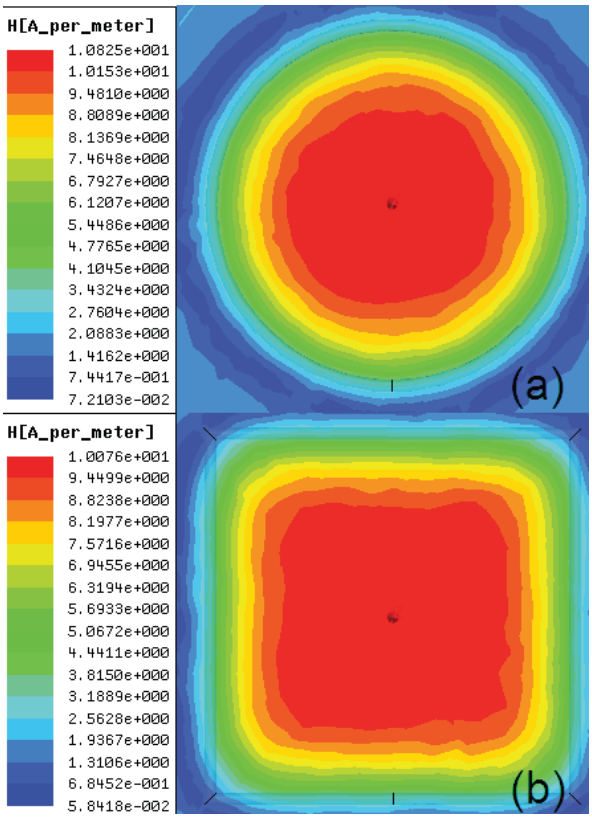

Fig. 5. A circular coil vs a polygonal coil in magnetic field intensity.

Helmholtz coil system will be needed to provide the microrobot with three-dimensional locomotion in the future.

III. Propulsion Experiments

A. Experimental Setup

A spiral-type microrobot was fabricated by winding a segment of wire around the outer surface of a dummy Pillcam SB2 capsules (Given Imaging). A permanent magnet (PM) was mounted at the capsule's center to obtain magnetic induction. It has a cylindrical shape with 6.35mm in diameter and 6.35mm in height. The magnetization of the NdBFe magnet was 6600G and oriented in the diametric direction of

Fig. 6. The endoscopic capsule attached with a spiral.

TABLE I
THE CAPSULES PREPARED FOR THE PROPULSION TESTS

Capsule No.	Number of spirals	Helical Angle	Spiral Height (mm)
1	1	5°	1
2	1	10°	1
3	1	15°	1
4	1	20°	1
5	2	20°	1
6	3	20°	1
7	1	10°	2

the capsule. Since every spiral structure, made of brass wire, was just wound on the cylindrical surface of the capsule, it had the same length (15 mm) in the longitudinal axis. The robotic capsule with one spiral is described in Fig. 6. Six robots of such with different spiral structures were made for the propulsion experiments, listed in Table 1.

A biaxial Helmholtz coil system was designed and constructed, as presented in Section II, for producing a rotating magnetic field. The axes of the two Helmholtz coils determined a plane, which was the rotational plane of field. The frozen intestinal specimen was defrosted a few hours before the experiments. Then, it was immersed in the physiological saline for some time, which was helpful to avoid tissue rupture. After that, the specimen, with the outer perimeter of ~41 mm, was located along the normal vector of the rotational plane of field. It was attached to two hollow plastic tubes and fixed at the both ends. The use of the hollow tubes makes it convenient for the robotic capsule to enter the small intestine afterwards. Along the intestine, some clips were used to simulate one of the physical functions of mesentery, stabilizing the intestine. The specimen was laid on a plastic plate, which was well leveled and mounted on an elevator platform. The experimental setup is shown in Fig. 7.

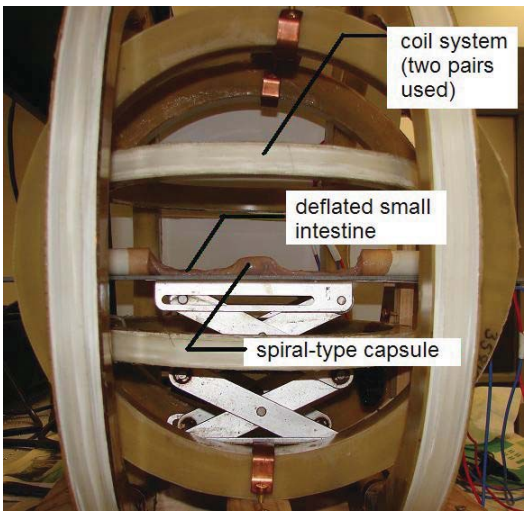

Fig. 7. General view of the experimental setup.

For each Helmholtz coil, the pair was connected in series to make sure the same current would flow through. Therefore, two signals were simultaneously required for the biaxial Helmholtz coil system. Matlab and an interface program named as QuaRC were utilized to generate the sinusoidal signals on the computer. These digital signals were sent to the data acquisition (DAQ) board (NI USB-6251) and converted to the analog outputs. Due to the use of this computer-based signal-generating system, amplitude and frequency as well as phase of a signal can be easily controlled. After that, the power supplies and the low-frequency power amplifiers were employed to augment the analog outputs to the AC current with the required magnitude, provided to the coil system to produce a rotating magnetic field. A schematic diagram of the system is described in Fig. 8.

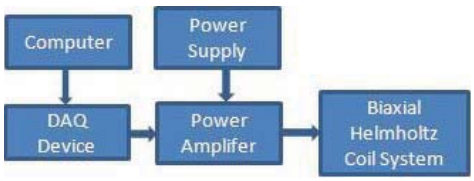

Fig. 8. Schematic diagram of the electromagnetic system.

Finally, a high-speed digital camera was used to record the motion of the spiral-type capsule for position recognition and propulsion analysis.

B. Experimental Procedures

Once the intestinal specimen was fixed as shown in Fig. 7, six capsules were tested one by one. For each capsule, it was inserted into the intestine from the hollow tube of one end. Then, the electromagnetic system was turned on to start a rotating magnetic field. The propulsion was recorded as a video by the camera. After that, the capsule was moved back to the starting position by reversing the rotation and then a rotating field of a different frequency was generated for a new test.

The small intestine could be dried out soon after being taken out of the fluid. Therefore, the experiments were carried out in a short time so that the tissue condition could be kept as consistent as possible. It is better not to spray a large mount of physiological saline during the tests since it may change the mechanical and tribological characteristics of the intestine. Only a little humidification was employed on the outer surface of the specimen when it was necessary.

C. Results

As the biaxial Helmholtz coil system was provided with the required AC currents, it was observed that the microrobot started to spin due to the magnetic torque. The robot kept spinning in synchronization with the rotating magnetic field. Thus, its rotational frequency was identical to the frequency of the input signals. It was propelled forward due to the presence of the spiral structure, which converted the rotation to a translational movement. The moving direction of the robotic capsule was normal to both axes of the Helmholtz coils and the deflated intestine swelled up where the capsule was located.

Fig. 9 shows the velocities of the capsules No. 1 ~ 4, which have one spiral and identical spiral height (1 mm) but different helical angles. From the graph, it is seen that the velocity increases for every capsule as the rotating frequency is raised. With the increase of helical angle from 5° to 15°, the propulsion velocity becomes higher. However, when the helical angle is raised to 20°, the propulsion velocity does not rise but becomes worse. At 5 Hz, its velocity is even smaller than the capsule with the helical angle of 10°. Therefore, the one with the helical angle of 15° performs best when only one spiral is employed for the capsule.

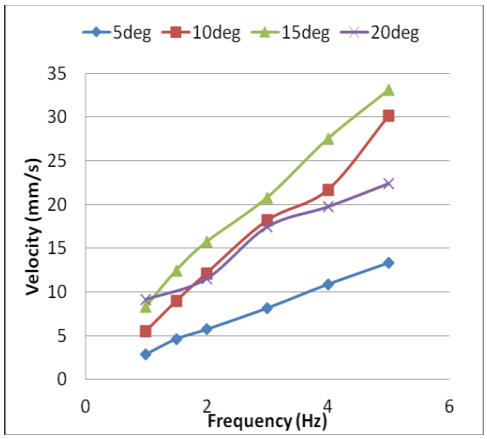

Fig. 9. Velocities of the capsules with one spiral and the same spiral height (1mm) but various helical angles.

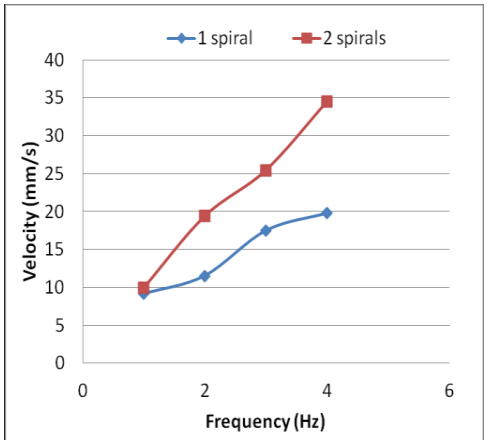

Fig. 10. Velocities of the capsules with the same spiral height (1mm) and helical angle (20°) but different number of spirals.

Fig. 10 shows the propulsive velocities of the capsules No. 4 and 5, which have the same spiral height (1 mm) and helical angles (20°) but different number of spirals. The graph indicates that the capsule with two spirals performs better than the capsule with one spiral, especially when the rotation becomes faster. The capsule with 3 spirals was also tested. However, due to the limitation of our amplifiers' power output, the generated magnetic torque was not high enough for the capsule to overcome the rotational friction. Therefore, the capsule No. 6 was not successfully propelled.

The capsule No. 7 with the spiral height of 2 mm also failed to be magnetically rotated since it was too thick for the intestinal specimen, causing a big deformation and consequently too large friction to overcome.

With the rotating frequency between 1 and 5 Hz, the propulsive velocities in the successful cases are in the range of 2.5 ~ 35 mm/s. Among all the tested capsules in this study, the capsule No. 5, with two spirals and helical angle of 20 and spiral height of 1 mm, shows the best performance with a propulsive velocity of 35 mm/s when rotating at 4 Hz

D. Discussions

As successfully propelled, the robotic capsule must lose some propulsion due to the slippery feature of the inner environment of the intestine. To investigate the slip effect, we introduce a parameter called the slip ratio, SR, which is given by,

$$SR = 1 - \frac{V_{real}}{Lf}, \tag{7}$$

where V_{real} is the real velocity, L is the lead of the spiral structure, and f is the rotational frequency. The denominator in Eq. 7 is the theoretical propulsion velocity for a spiral-type capsule without any slip.

Fig. 11 shows the examples of SR for the capsules No. 3 (1 spiral, helical angle = 15°) and 4 (1 spiral, helical angle = 20°). It is observed that the slip ratio increases with the rise of the frequency, which means more propulsion is lost when the rotation becomes faster because of the slip. By comparing the SRs for the two capsules, it is suggested that bigger helical angle leads to more slip for those capsules with only one spiral. Theoretically, the bigger helical angle should be more helpful to convert effective rotational movement to translational movement. However, if this increased conversion is not able to make up for the lost propulsion resulted from the increased slip, the propulsive velocity may decrease instead of increasing. We postulate that too much slip is probably the reason why the capsule No. 4 performs worse than the capsule No. 3, shown in Fig. 9. The introduction of more spirals can overcome this problem. Fig. 12 shows the examples of SR for the capsules No. 4 (1 spiral, helical angle = 20°) and No. 5 (2 spiral, helical angle = 20°). It is obvious that the capsule with two spirals has much less slip than the capsule with one spiral.

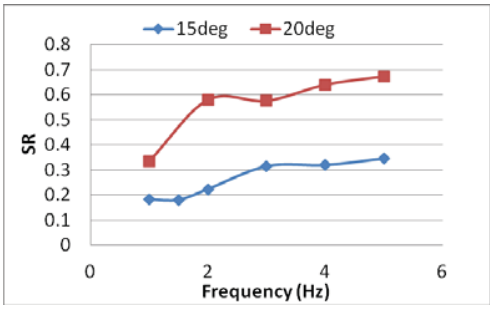

Fig. 11. The examples of SR for the capsules No. 3 and 4.

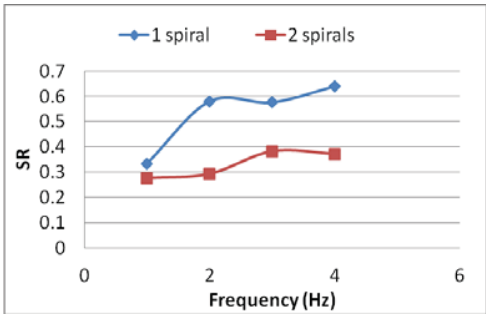

Fig. 12. The examples of SR for the capsules No. 4 and 5.

As reported before [15], a spiral-type microrobot depends on the pressure difference between two sides of the spiral to generate propulsion. The pressure is essentially the internal

pressure of the intestinal tract, which was mostly determined by its deformation due to the capsule's insertion. The addition of the spiral makes the cross-section of the robotic capsule bigger, which increases the deformation of the intestinal tract. This increase gets larger if the helical angle is smaller. Therefore, when the number of spiral and spiral height are the same, a smaller helical angle leads more deformation in the intestine and consequently causes more internal pressure. Increasing the number of spirals or spiral height causes the same effect. Once the pressure increases, there is more support from the intestinal wall, which reduces the slip of the capsule. However, this rise of pressure also increases the friction in both rotational and translational directions, requiring more power for the propulsion.

IV. Conclusion

A magnetic propulsion system is built to provide active locomotion to a spiral-type endoscopic microrobot. Magnetic modeling was conducted to predict the distribution of magnetic field. The analysis shows that a circular Helmholtz coil can produce higher field intensity than a polygonal Helmholtz coil when they have comparable dimensions and are applied the same electrical current. This theoretical analysis of the magnetic system is helpful for the design and construction of an external electromagnetic system for providing wireless power to a robotic agent.

With the biaxial Helmholtz coil system, several magnetic spiral-type capsules were propelled inside a real small intestine. The rotating frequencies from 1 Hz to 5 Hz were applied in turn. The propulsive velocities were in the range of 2.5 ~ 35 mm/s. For each capsule, it moves faster as the frequency increases, as expected. In terms of the effect of helical angle, as it rises from 5° to 15°, the propulsive velocity increases. However, when the helical angle is raised to 20°, the propulsive velocity is reduced. The slip effect is investigated that a higher helical angle may increase the slip ratio due to the reduced internal pressure as a result of the reduced deformation of the intestinal tract. Hence, though a larger helical angle helps to effectively convert more rotation to translation, it may be detrimental to the propulsion if the increased conversion rate cannot offset the side effect caused by the increased slip. Although reducing the rotating speed can make the slip smaller, it simultaneously reduces the propulsion velocity as well. To overcome this problem, both increasing number of spirals and spiral height may be effective. However, they should be carefully chosen based on the size of the intestine and the power output of the external system such that enough torque can be generated for the rotation. Among all the fabricated capsules in this study, the capsule No. 5, with one spiral and helical angle of 20° and spiral height of 1 mm, shows the best performance.

Further work will aim more experiments with more intestinal specimens to increase the generality of the results presented in this paper. Different materials will be employed as spirals to investigate the impact of their properties on propulsion in the small intestine. Meanwhile, viscoelastic modeling will be carried out to reasonably predict the propulsion and help the design and establishment of a performance-optimized spiral-type microrobot.

Acknowledgment

The authors are grateful to Given Imaging Pty. Ltd (Sydney) for providing the capsules used in this study.

References

[1] B. J., Nelson, I. K. Kaliakatsos and J. J. Abbott, "Microrobots for minimally invasive medicine," *Annu. Rev. Biomed. Eng.,* vol. 12, pp. 55–85.

[2] G. Iddan, G. Meron, A. Glukhovsky and P. Swain, "Wireless capsule endoscope," *Nature*, vol. 405, pp. 417–418, May 2000.

[3] A. Moglia, A. Menciassi, P. Dario and A. Cuschieri, "Capsule endoscopy: progress update and challenges ahead," *Nat. Rev. Gastroenterol. Hepatol.*, vol. 6, pp. 353–362, 2009.

[4] A. Moglia, A. Menciassi and P. Dario, "Recent Patents on wireless capsule endoscopy," *Recent Patents Biomed. Eng.*, vol. 1, pp. 24-33, 2008.

[5] J. L. Toennies, G. Tortora, M. Simi and et al., "Swallowable medical devices for diagnosis and surgery: the state of the art," *Proceedings of the Institution of Mechanical Engineers, Part C: Journal of Mechanical Engineering Science*, vol. 224, pp. 1397-1414, 2010.

[6] D. Hosokawa, T. Ishikawa, H. Morikawa and et al., "Development of a biologically inspired locomotion system for a capsule endoscope," *Int J Med. Robot*., vol. 5, pp. 471-478, 2009.

[7] H. M. Kim, S. Yang, J. Kim and et al., "Active locomotion of a paddling-based capsule endoscope in an in vitro and in vivo experiment," *Gastrointestinal Endoscopy*, vol. 72, pp. 381-387, 2010.

[8] P. Valdastri, III R. J. Webster, C. Quaglia and et al., "A new mechanism for mesoscale legged locomotion in compliant tubular environments," IEEE Transactions on *Robotics*, vol. 25, pp. 1047-1057, 2009.

[9] S. H. Woo, T. W. Kim and J. H. Cho, "Stopping mechanism for capsule endoscope using electrical stimulus," *Medical and Biological Engineering and Computing*, vol. 48, pp. 97-102, 2010.

[10] G. Tortora, P. Valdastri, E. Susilo and et al., "Propeller-based wireless device for active capsular endoscopy in the gastric district," *Minimally Invasive Therapy and Allied Technologies*, vol. 18, pp. 280-290, 2009.

[11] H. Zhou, G. Alici, W. Li and S. Ghanbar, "Experimental characterization of a robotic drug delivery system based on magnetic propulsion," 2011 IEEE/ASME International Conference on *Advanced Intelligent Mechatronics (AIM)*, pp. 209-214, 2011.

[12] F. Carpi, N. Kastelein, M. Talcott and C. Pappone, "Magnetically controllable gastrointestinal steering of video capsules," *IEEE Transactions on Biomedical Engineering*, vol. 58, pp. 231-234, 2011.

[13] M. Gao, C. Hu, Z. Chen, H. Zhang and S. Liu, "Design and fabrication of a magnetic propulsion system for self-propelled capsule endoscope," *IEEE Transactions on Biomedical Engineering*, vol. 57, pp. 2891-2902, 2010.

[14] M. Sendoh, K. A. Yamazaki, A. Chiba, M. Soma, K. Ishiyama and K. I. Arai, "Spiral type magnetic micro actuators for medical applications," In Proceedings of the International Symposium on *Micro-NanoMechatronics and Human Science*, pp. 319-324, 2004.

[15] Y. Zhang, S. Jiang, X. Zhang, X. Ruan and D. Guo, "A variable-diameter capsule robot based on multiple wedge effects," *IEEE/ASME Transactions on Mechatronics*, vol. 16, pp. 241-254, 2011.

[16] H. D. Hoeg, A. B. Slatkin, J. W. Burdick, "Biomedical modeling of the small intestine as required for the design and operation of a robotic endoscope," In Proceedings of the 2000 IEEE International Conference on *Robotics and Automation*, pp. 1599-1606, 2000.

[17] D. Jiles, *Introduction to magnetism and magnetic materials*, 2nd Edition. London: Chapman & Hall, 1998.

[18] ANSYS, Inc., Maxwell 3D Technical Notes, http://www.ansoft.com/products/em/maxwell/.